Onur Sayman*, Mustafa Ozen, Adnan Ozel, Teyfik Demir and Behiye Korkmaz

A non-linear elastic-plastic stress analysis in a ductile double-lap joint

Abstract: In this study, an elastic-plastic stress analysis was proposed in order to obtain shear stress distribution in a double-lap joint, analytically. The solution was carried out using incremental theory. The obtained shear stress was then used for determining the peel stress in the adhesive. The elastic peel stress distribution in the adhesive was determined using Newton-Raphson method. In this study, FM73 (Cytec Industries Inc., New Jersey, USA) ductile adhesive was selected as it represents plastic hardening. The analytical results were compared with the finite element solution. For that, ANSYS 10 Software (Figes Engineering A.S., Turkey) was used so as to compare with the analytical results. A good agreement was obtained between the two methods.

Keywords: analytical solution; double-lap joint; elastic-plastic stress analysis; finite element solution; peel stress.

***Corresponding author: Onur Sayman**, Engineering Faculty, Department of Mechanical Engineering, Dokuz Eylul University, Bornova, Izmir, Turkey, e-mail: onur.sayman@deu.edu.tr
Mustafa Ozen: Engineering Faculty, Department of Mechanical Engineering, Dokuz Eylul University, Bornova, Izmir, Turkey
Adnan Ozel: Engineering Faculty, Department of Mechanical Engineering, Ataturk University, Erzurum, Turkey
Teyfik Demir: Department of Mechanical Engineering, TOBB University of Economics and Technology, Sogutozu, Ankara, Turkey
Behiye Korkmaz: Engineering Faculty, Department of Mechanical Engineering, Uludag University, Gorukle, Bursa, Turkey

1 Introduction

Adhesively bonded joints have been used in several applications. Adhesive bonding usually enables structures to have lower cost and weight in comparison with the conventional methods. The adhesive bonding offers certain advantages over traditional joining techniques, such as corrosion, fatigue resistance, crack retardation, cost saving and lighter weight of structural component. It also enables to joint dissimilar materials effectively in comparison with the conventional methods. This method is especially suitable for the joining of thin materials. To satisfy the safety of adhesively bonded joints, it is necessary to estimate a correct stress distribution in the joints. A ductile adhesive ensures high strengths in the joints, by using the ductile properties and residual stresses in the joints. An explicit analytical solution is presented in double-lap joints by Smith [1]. He reported the plastic shear stress in the adhesive. He also determined the peel stresses in the adhesive. Silva and Adams [2] proposed a technique for decreasing the peel stresses in double joints and to increase the joint strength, particularly at low temperatures. Kadioglu et al. [3] studied a very ductile adhesive and a structural epoxy. It has been shown that when designed correctly, the ductile adhesive could take advantage of the epoxy, and that an adhesive which is relatively stronger in one mode (e.g., tension) is not necessary so far in the other mode (e.g., bending). Four-point bending tests were performed in this study. Apalak and Gunes [4] investigated three-dimensional elastic stresses in an adhesively bonded single-lap joint with functionally graded adherends in tension. A finite layered solid element was formulated based on three-dimensional elasticity. Silva and Adams [5] carried out a finite element model to design a joint, suitable for use from low to high temperatures. They studied shear and peel stresses in the adhesive so as to find the best possible joint design. Xiao et al. [6] presented an analytical solution for the in-plane stiffness response of adhesively bonded double-lap shear joints. Her [7] developed an analytical solution for finding the shear stress in single-lap and double-lap joints. Schmidt and Edlund [8] proposed a finite element method so as to analyze the failure of adhesively bonded structures. Kadioglu et al. [9] measured shear stress-strain behavior of two low modulus structural adhesives using the butt-torsion test. The Nadai correction for nonlinear shear behavior was utilized in the solutions. Chataigner et al. [10] proposed a procedure using nonlinear failure criteria for double-lap bonded joints. The proposed analytical procedure is based on the well-known Shear Lag Theory of Volkersen. Edlund et al. [11] studied a model for an adhesively bonded joint with elastic-plastic adherends and a softening adhesive. Malvade et al. [12] studied the simulation of non-linear mechanical behaviors of adhesively bonded double-lap joints for variable extension rates and temperatures using the implicit ABAQUS solver. Sayman [13] proposed an analytical model for the elasto-plastic solution of a single-lap joint. DP 460 (3M Scotch-Weld

Epoxy Adhesives, Turkey) ductile adhesive was used and ANSYS finite element solution was carried out for the numerical solution. Markofelas and Papathanassiou [14] developed a shear-lag model in order to evaluate stress redistributions in double-lap joints under axial lap-shear cyclic loading. The adherend materials exhibit linear elastic behavior; however, the adhesive material provides the elastic-perfectly plastic shear stress-strain relation.

In this study, an elastic-plastic stress analysis was carried out in a ductile double-lap joint. The shear and peel stresses in the adhesive were found analytically. The results were compared with the finite element solution.

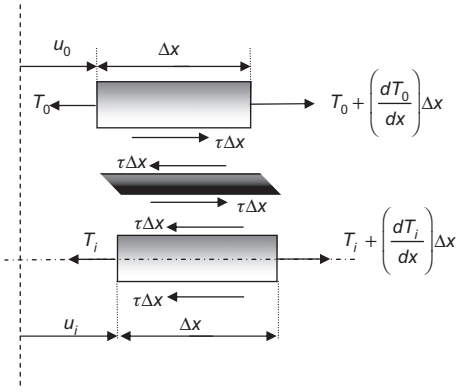

Figure 2 Free body-diagrams of the joint.

2 Mathematical formulation

The geometric structure of a double-lap joint is shown in Figure 1. Free body-diagrams of the joints are shown in Figure 2. The static equilibrium yields the following equations as

$$\frac{dT_0}{dx}+\tau=0 \tag{1}$$

$$\frac{dT_i}{dx}-2\tau=0 \tag{2}$$

where T_0 and T_i are the tensions per unit width in adherends, respectively. The shear strain in the adhesive is written as

$$\varepsilon_{xy}=\frac{1}{2\eta}(u_i-u_0) \tag{3}$$

The derivation of ε_{xy} gives the relation

$$\frac{d\varepsilon_{xy}}{dx}=\frac{1}{2\eta}\left(\frac{du_i}{dx}-\frac{du_0}{dx}\right)=\frac{1}{2\eta}(\varepsilon_i-\varepsilon_0)=\frac{1}{2\eta}\left(\frac{T_i}{E_it_i}-\frac{T_0}{E_0t_0}\right) \tag{4}$$

If the incremental theory is used in the solution, $d\varepsilon_{xy}$ can be written as

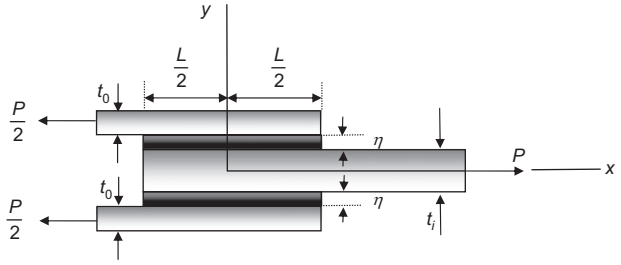

Figure 1 Geometric structure of a double-lap joint.

$$d\varepsilon_{xy}=d\varepsilon_{xy}^e+d\varepsilon_{xy}^p=\frac{d\tau}{2G_a}+\tau d\lambda \tag{5}$$

where η and G_a are the thickness and the shear modulus of the adhesive, respectively.

$$\frac{d\varepsilon_{xy}}{dx}=\frac{d\tau}{2G_a dx}+\frac{\tau d\lambda}{dx} \tag{6}$$

The Ludwik equation for the shear stress is written as

$$\tau=\tau_0+K\gamma_p^n \tag{7}$$

In the solution, n is chosen as 1, for an easy analytical solution, because for $n\neq1$, the analytical solution may be impossible or very difficult. The solution for $n=1$ is almost close to reality. However, a more realistic solution can be obtained by using the nonlinear stress-strain diagrams for $n=0.597$. Therefore, nonlinear ANSYS solutions have been added to the shear stress diagrams along the joints in Figures 3–5. $d\varepsilon_{xy}^p$ can be expressed in terms of the equivalent strain $d\gamma^p$ as

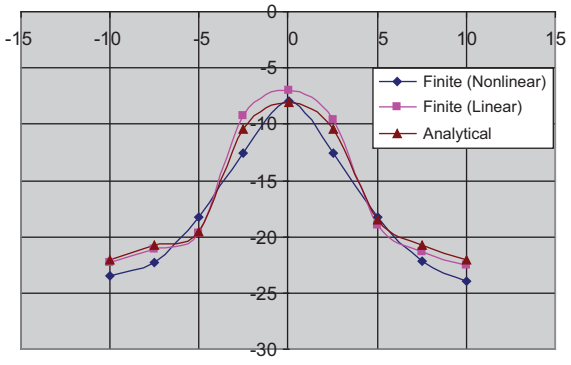

Figure 3 Shear stress along the adhesive for $t_0=1.6$ mm.

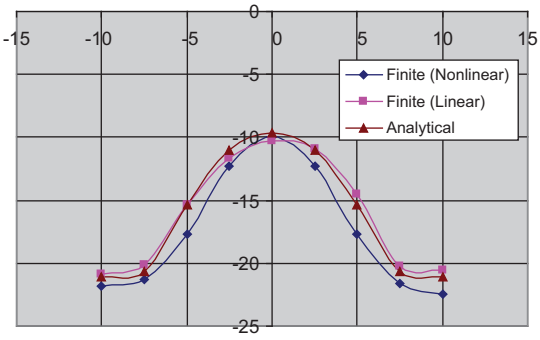

Figure 4 Shear stress along the adhesive for t_0=2.4 mm.

$$d\gamma^p=\frac{\sqrt{6}}{3}d\varepsilon_{xy}^p \tag{8}$$

and

$$\frac{d\varepsilon_{xy}^p}{dx}=\frac{3}{\sqrt{6}}\frac{d\tau}{Kdx} \tag{9}$$

The total strain increment is

$$\frac{d\varepsilon_{xy}}{dx}=\frac{d\tau}{dx}\left(\frac{1}{2G_a}+\frac{3}{\sqrt{6}K}\right)=\frac{1}{2\eta}\left(\frac{T_i}{E_it_i}-\frac{T_0}{E_0t_0}\right) \tag{10}$$

From this equation,

$$\frac{d\tau}{dx}=b\left(\frac{T_i}{E_it_i}-\frac{T_0}{E_0t_0}\right) \tag{11}$$

where

$$b=\frac{1}{2\eta\left(\frac{1}{2G_a}+\frac{3}{\sqrt{6}K}\right)} \tag{12}$$

Static equilibrium is written as

$$P=T_i+2T_0 \quad \text{and} \quad T_i=P-2T_0 \tag{13}$$

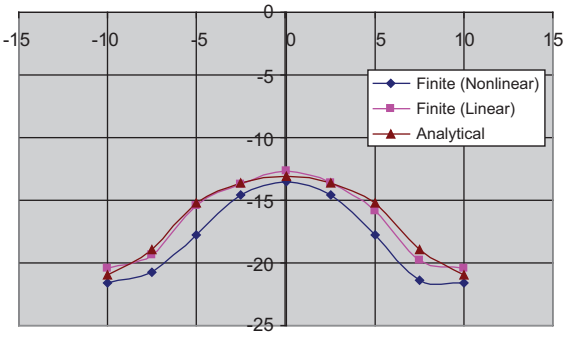

Figure 5 Shear stress along the adhesive for t_0=3.2 mm.

Putting in the equation of T_0 yields the equation

$$\frac{d^2T_0}{dx^2}-\lambda_p^2T_0=-\frac{bP}{E_it_i} \tag{14}$$

where

$$\lambda_p^2=b\left(\frac{2}{E_it_i}+\frac{1}{E_0t_0}\right) \tag{15}$$

The boundary conditions are

$$T_0=0;\quad x=\frac{L}{2} \tag{16}$$

$$T_0=\frac{P}{2};\quad x=-\frac{L}{2} \tag{17}$$

where L is the total length of the adhesive. The solution of this differential equation produces the plastic shear stress in the adhesive as

$$\tau=\frac{P\lambda_p}{4}\left[\frac{\cosh\left(\lambda_p x\right)}{\sinh\left(\frac{\lambda_p L}{2}\right)}-\frac{E_it_i-2E_0t_0}{\left(E_it_i+2E_0t_0\right)}\frac{\sinh\left(\lambda_p x\right)}{\cosh\left(\frac{\lambda_p L}{2}\right)}\right] \tag{18}$$

In the elastic region, the shear stress can be found from the work of Her [7].

2.1 Peel stress

The peel stress is another important stress component in the adhesive. However, in this study, the solution of the peel stress is found individually. The shear stress distribution along the adhesive is obtained first. Then it is substituted in the solution of the peel stress, as shown in Figure 6.

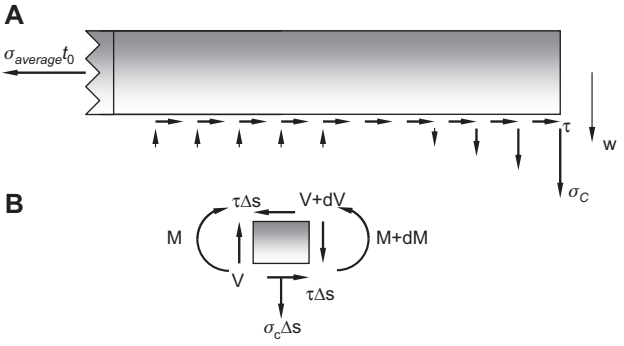

Figure 6 Outer adherend. (A) Stresses, (B) element loads.

The equations of the peel stress are presented by Smith [1]. They are

$$\frac{dM}{dx}=V-\tau\frac{t_0}{2} \quad \text{and} \quad \frac{dV}{dx}=-\sigma_c \tag{19}$$

and the other equations

$$\frac{d^2w_0}{dx^2}=-\frac{M}{D} \quad \text{and} \quad \frac{\sigma_c}{E_a}=-\frac{w_0}{\eta} \tag{20}$$

where M, V, w_0 and σ_c are the bending moment, shear force, deflection and peel stress, respectively. These equations produce a basic differential equation which is

$$D\frac{d^4w_0}{dx^4}-\frac{E_aw_0}{\eta}=\frac{t_0}{2}\frac{d\tau}{dx} \tag{21}$$

Dividing both sides by D yields

$$\frac{d^4w_0}{dx^4}-\frac{E_aw_0}{D\eta}=\frac{t_0}{2D}\frac{d\tau}{dx} \tag{22}$$

and

$$\frac{d^4w_0}{dx^4}-X^4w_0=\frac{t_0}{2D}\frac{d\tau}{dx} \tag{23}$$

where

$D=\frac{E_0t_0}{12\left(1-v_0^2\right)}$, $X^4=\frac{E_a}{4D\eta}$, and v_0 is the Poisson's ratio of the outer adherent. The solution of the homogenous part is given by Smith [1] under the condition of $\frac{d\tau}{dx}=0$.

$$w_h=A\sin Xx\cos\text{h}\,Xx+B\cos Xx\sin\text{h}\,Xx+C\sin Xx\sin\text{h}\,Xx+F\cos Xx\cos\text{h}\,Xx \tag{24}$$

However, in this study, $\frac{d\tau}{dx}$ is taken to be different from the zero. Then the private solution of the equation in the plastic region of the shear stress Eq. (18) is added as

$$w_p=C_1\cos\text{h}(\lambda_px)+C_2\sin\text{h}(\lambda_px) \tag{25}$$

Eq. (23) is rearranged in Eq. (25) as follows:

$$C_1\cos\lambda_p^4\cos\text{h}\left(\lambda_px\right)+C_2\lambda_p^4\sin\text{h}\left(\lambda_px\right)-X^4\left(C_1\cos\text{h}\left(\lambda_px\right)+C_2\sin\text{h}\left(\lambda_px\right)\right)=\frac{t_0}{2D}\frac{P\lambda_p^2}{4}\left[\frac{\sin\text{h}\left(\lambda_px\right)}{\sin\text{h}\left(\frac{\lambda_pL}{2}\right)}-\frac{E_it_i-2E_0t_0}{E_it_i+2E_0t_0}\frac{\cos\text{h}\left(\lambda_px\right)}{\cos\text{h}\left(\frac{\lambda_pL}{2}\right)}\right] \tag{25a}$$

After the solution of Eq. (25a), the constants are found as

$$C_1=\frac{s\lambda_p}{\lambda_p^4-X^4}\frac{P\lambda_p}{4}\left[-\frac{E_it_i-2E_0t_0}{E_it_i+2E_0t_0}\frac{1}{\cos\text{h}\left(\frac{\lambda_pL}{2}\right)}\right] \tag{26}$$

$$C_2=\frac{s\lambda_p}{\lambda_p^4-X^4}\frac{P\lambda_p}{4\sin\text{h}\left(\frac{\lambda_pL}{2}\right)} \tag{27}$$

λ_p is given by Eq. (15), where

$$s=\frac{t_0}{2D} \tag{28}$$

When the shear stress is elastic, the elastic shear stress equation found from the work of Her [7] is substituted in the above equation instead of the plastic relation in Eq. (25). The boundary conditions are

$$M=-D\frac{d^2w_0}{dx^2}=0 \text{ at } x=\pm\frac{L}{2} \tag{29}$$

and

$$V=0, \quad \text{where} \quad \frac{dM}{dx}=-\tau\frac{t_0}{2}=-D\frac{d^3w_0}{dx^3} \quad \text{at} \quad x=\frac{L}{2} \tag{30}$$

The other relation is

$$\int_{-\frac{L}{2}}^{\frac{L}{2}}\sigma_c dx=\int_{-\frac{L}{2}}^{\frac{L}{2}}w_0dx=0 \tag{31}$$

As the peel stress (σ_c) is produced by the bending moment, the summation of the peel stress along the adhesive is equal to zero. Therefore, the peel stress satisfies the zero. As a result of this, the summation of the deflection (w_0) along the adhesive is equal to zero, due to the linear relation between them [Eq. (20)]. The unknown integration constants are taken out from the boundary conditions and then are put in Eq. (31) in terms of the constant A. The numerical solution is carried out for Eq. (31). For that, the numerical integration is performed by Newton-Cotes formulas, and then w_0 is calculated by using the Newton-Raphson method. Subsequently, the peel stress σ_c is found along the adhesive at each point, numerically.

3 Results and discussions

In this study, composite plates were manufactured by the vacuum infusion method. Material properties are given in

E_x (MPa)	E_y (MPa)	υ_{xy}	G_{xy}
33,000	10,500	0.27	4800

Table 1 Mechanical properties of composite adherends.

E_a (MPa)	υ	τ_y (MPa)	K (MPa)	n
4200	0.35	17.0	40.4	1

Table 2 Mechanical properties of adhesive.

Table 1. The adhesive joint is a ductile material, namely FM-73. An external force is applied to the double-lap joint. Then the τ–γ diagram is obtained, as shown in Figure 7. Material properties of the adhesive were found from this diagram. The yield point of the shear stress is τ_y=17.0 MPa and the plasticity constants are K=40.4 MPa and n=1. The true stress-strain values are used in the construction of the diagram. Mechanical properties of the adhesive are given in Table 2.

The magnitude of P is chosen as 640 N. The length and thickness of the adhesive are 20 mm and 0.14 mm, respectively. t_0 is selected as 1.6, 2.4 and 3.2 mm. t_i is chosen as $2t_0$, in each case.

The finite element analysis was carried out for the numerical solution. Solid 182 element of four nodes was utilized in the numerical analysis. Symbolic meshing of the double-lap joint is shown in Figure 8. This numerical solution provides a two-dimensional stress analysis. However, the analytical stress analysis is performed for the one-dimensional case.

The shear stress along the adhesive for t_0=1.6 mm is shown in Figure 3. As seen in this figure, analytical and numerical solutions give close results along the adhesive. The analytical result of the shear stress at the ends is a little bit greater than the numerical solution. The analytical and numerical results are the greatest at the ends of the adhesive.

The shear stress along the adhesive for t_0=2.4 mm is shown in Figure 4. As seen in the figure, both the analytical and numerical solutions are in good agreement. They are highest at the ends of the adhesive.

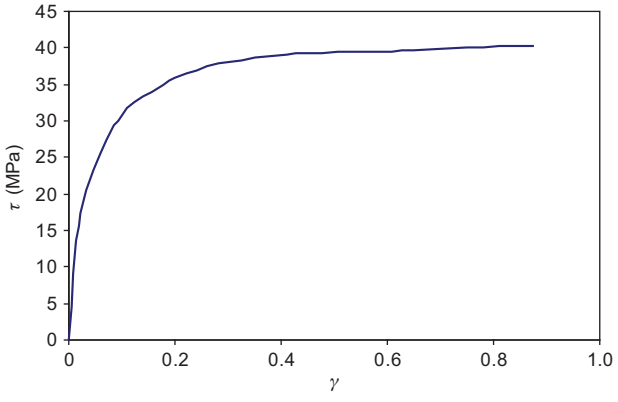

Figure 7 τ–γ diagram of the FM-73 adhesive.

The shear stress distribution along the adhesive for t_0=3.2 mm is shown in Figure 5. As seen in the figure, shear stress is the highest at the ends of the adhesive. It is similar for both analytical and numerical solutions.

The peel stress distribution along the adhesive for t_0=1.6 mm is shown in Figure 9. It is seen that both analytical and numerical solutions satisfy close results. The peel stress is compressive and tensile at the left-hand and right-hand sides, respectively. The magnitude of the tensile peel stress at the right-hand side is higher than that of the compressive peel stress at the left-hand side.

The peel stress distribution along the adhesive for t_0=2.4 mm is shown in Figure 10. Both the analytical and numerical solutions produce close results. The peel stress is the highest at the ends of the adhesive. The magnitude of the peel stress at the right-hand side is higher than that at the left-hand side. It is compressive and tensile at the left-and right-hand sides, respectively.

The peel stress distribution along the adhesive for t_0=3.2 mm is shown in Figure 11. It is seen that both the analytical and numerical solutions provide close results. The peel stress is tensile and compressive at the right-hand

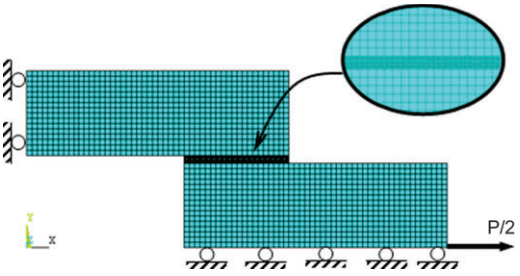

Figure 8 Symbolic modeling and meshing of the double-lap joint.

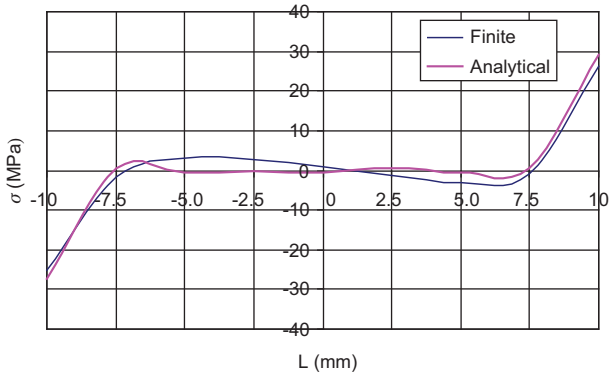

Figure 9 Peel stress distribution along the adhesive for t_0=1.6 mm.

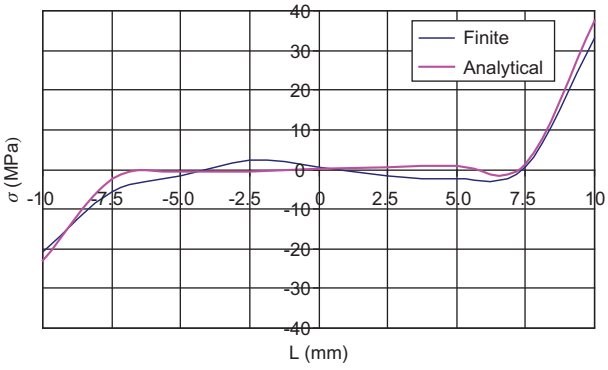

Figure 10 Peel stress distribution along the adhesive for t_0=2.4 mm.

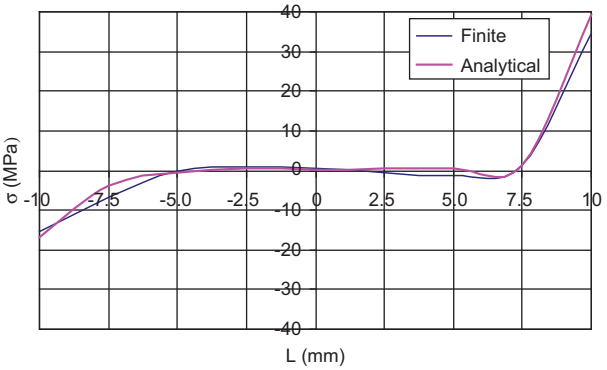

Figure 11 Peel stress distribution along the adhesive for t_0=3.2 mm.

and left-hand sides, respectively. The magnitude of the tensile peel stress is higher than that at the left-hand side.

It is also seen that when the thickness of t_0 is chosen to be thin, the peel stress for both solutions obtained are very close, due to the small bending moments. As the thicknesses (t_0 and t_i) are small, the bending moment also becomes small. The small bending moment produces small peel stress. Smith [1] proposed a relation for sufficiently long adhesives; the maximum peel stress in this kind of adhesive is

$$\sigma_{C\max}=\frac{E_a\tau\ t_0}{\eta 2D2X^3} \tag{32}$$

where E_a is the Young's Modulus of the adhesive. The magnitude of the highest peel stress at the ends of the joints is obtained approximately as 28.52, 32.26 and 37.40 MPa from Eq. (32), for t_0=1.6, 2.4, and 3.2 mm, respectively. These results are close to the theoretical and numerical solutions. In all the adhesives, the shear stress exceeds the yield point of the adhesive; when the external force is released, the residual stress occurs in the adhesive. The load carrying capacity of the joints can be increased by using the residual stress.

4 Conclusions

In this study, a nonlinear stress analysis was carried out in a double-lap joint. Shear and peel stresses are found by theoretical and numerical methods.

a. The shear stress components in the adhesive can be obtained analytically and numerically.
b. The shear stress component was obtained to be the highest at the ends of the adhesive for both solutions.
c. Both analytical and numerical methods produce peel stress closer in thin t_i and t_0 adherends.
d. The peel stress is an important component together with the shear stress in the failure of adhesive.
e. Analytical and numerical methods yield good agreement in the analysis of the shear stress.
f. The strength of the joint can be increased by releasing the external force and obtaining the residual stresses in a ductile adhesive.

Received July 10, 2012; accepted November 16, 2012; previously published online December 17, 2012

References

[1] Smith LJH. *Adhesive-Bonded Double-Lap Joints*. National Aeronautics and Space Administration, Langley Research Center: Hampton, 1973.
[2] Silva LFM, Adams RD. *Int. J. Adhes. Adhes.* 2007, 27, 227–235.
[3] Kadioglu F, Ozel A, Sadeler R, Adams RD. *J. Adv. Mater.* 2003, 35, 47–51.
[4] Apalak MK, Gunes R. *Compos. Struct.* 2005, 70, 444–467.
[5] Silva LFM, Adams RD. *Int. J. Adhes. Adhes.* 2007, 27, 362–379.
[6] Xiao X, Foss PH, Schroeder JA. *Int. J. Adhes. Adhes.* 2004, 24, 229–237.
[7] Her SC. *Compos. Struct.* 1999, 47, 673–678.
[8] Schmidt P, Edlund U. *Int. J. Adhes. Adhes.* 2010, 30, 665–681.
[9] Kadioglu F, Adams RD, Guild FJ. *J. Adhesion* 2000, 73, 117–133.
[10] Chataigner S, Caron JF, Diaz AD, Aubagnac C, Benzarti K. *Int. J. Adhes. Adhes.* 2010, 30, 10–20.
[11] Edlund U, Schmidt P, Roguet E. *Comput. Methods Appl. Mech. Eng.* 2009, 198, 740–752.
[12] Malvade I, Deb A, Biswas P, Kumar A. *Comput. Mater. Sci.* 2009, 44, 1208–1217.
[13] Sayman O. *Composites, Part B* 2012, 43, 204–209.
[14] Markofelas SI, Papathanassiou TK. *Int. J. Adhes. Adhes.* 2009, 29, 737–744.